

Experimental Schmidt Decomposition and State Independent Entanglement Detection

Wiesław Laskowski,^{1,2,3} Daniel Richart,^{2,3} Christian Schwemmer,^{2,3} Tomasz Paterek,⁴ and Harald Weinfurter^{2,3}

¹*Institute of Theoretical Physics and Astrophysics, University of Gdańsk, PL-80-952 Gdańsk, Poland*

²*Max-Planck-Institut für Quantenoptik, Hans-Kopfermann-Strasse 1, D-85748 Garching, Germany*

³*Department für Physik, Ludwig-Maximilians-Universität, D-80797 München, Germany*

⁴*Centre for Quantum Technologies, National University of Singapore, 3 Science Drive 2, 117543 Singapore, Singapore*

(Received 17 November 2011; revised manuscript received 6 April 2012; published 11 June 2012)

We introduce an experimental procedure for the detection of quantum entanglement of an unknown quantum state with a small number of measurements. The method requires neither *a priori* knowledge of the state nor a shared reference frame between the observers and can thus be regarded as a perfectly state-independent entanglement witness. The scheme starts with local measurements, possibly supplemented with suitable filtering, which essentially establishes the Schmidt decomposition for pure states. Alternatively we develop a decision tree that reveals entanglement within few steps. These methods are illustrated and verified experimentally for various entangled states of two and three qubits.

DOI: [10.1103/PhysRevLett.108.240501](https://doi.org/10.1103/PhysRevLett.108.240501)

PACS numbers: 03.67.Mn, 03.65.Ta, 03.67.Bg, 42.50.Ex

Introduction.—Entanglement is the distinguishing feature of quantum mechanics and it is the most important resource for quantum information processing [1,2]. For any experiment it is thus of utmost importance to easily reveal entanglement, ideally with as little effort as possible. Common methods suffer from disadvantages. On the one hand, employing the Peres–Horodecki criterion [3,4] or evaluating entanglement measures, one can identify entanglement in arbitrary states; however, it requires full state tomography. On the other hand, various entanglement witnesses [4–10] can be determined with much fewer measurements, but they give conclusive answers only if the state under investigation is close to the witness state; i.e., they require *a priori* knowledge.

Recently, it has been shown that the existence of entanglement can be inferred from analyzing correlations among the measurement results on the subsystems of a quantum state. The properly weighted sum of correlations will overcome characteristic thresholds only if the state is entangled [11]. Here we further develop this approach to obtain a simple and practical method to detect entanglement of all pure states and some mixed states by measuring only a small number of correlations. Since the method is adaptive, it does not require *a priori* knowledge of the state nor a shared reference frame between the possibly remote observers, and thus it greatly simplifies the practical application. We describe two schemes. The first one essentially can be seen as a direct implementation of Schmidt decomposition, which identifies the maximal correlation directly. For bipartite pure systems, this approach can be divided conceptually into two stages: (i) calibration that establishes the experimental Schmidt decomposition [12,13] of a pure state by local measurements and suitable filtering and (ii) two correlation measurements to verify the entanglement criterion. The second scheme shows how to use a

decision tree to obtain a rapid violation of the threshold, thereby identifying entanglement.

Entanglement criterion.—For a two-qubit quantum state ρ , Alice and Bob observe correlations between their local Pauli measurements σ_k and σ_l , respectively. They are defined as the expectation values of the product of the two measurements, $T_{kl} = \text{Tr}[\rho(\sigma_k \otimes \sigma_l)]$, with the so-called correlation tensor elements $T_{kl} \in [1, -1]$. The local values T_{k0} (T_{0l}), with σ_0 being the identity operator, form the local Bloch vector of Alice (Bob). Using these measurements, a sufficient condition for entanglement can be formulated as [11,14]:

$$\sum_{k,l=x,y,z} T_{kl}^2 > 1 \Rightarrow \rho \text{ is entangled.} \quad (1)$$

For pure states this is also a necessary condition, while for mixed states care has to be taken. For mixed states, the likelihood of detecting the entanglement decreases with purity [15]. An extension of (1) can generally identify entanglement of an arbitrary mixed state, however, then losing the state independence [11,16]. Note two important facts. First, Eq. (1) can be seen as a state-independent entanglement witness, derived without any specific family of entangled states in mind. Second, to test whether the state is entangled, it is sufficient to break the threshold; i.e., it is neither required to measure all correlations nor to compute the density matrix [17]. Rather, it is now the goal to find strategies that minimize the number of correlation measurements. We show how this can be done by a particularly designed decision tree, or by identifying a Schmidt decomposition from local results and filtering when necessary.

Schmidt decomposition.—Consider pure two-qubit states. Any such state has a Schmidt decomposition

$$|\psi_S\rangle = \cos\theta|a\rangle|b\rangle + \sin\theta|a_\perp\rangle|b_\perp\rangle, \quad \theta \in \left[0, \frac{\pi}{4}\right], \quad (2)$$

where the coefficients are real and the local bases $\{|a\rangle, |a_\perp\rangle\}$ and $\{|b\rangle, |b_\perp\rangle\}$ are called the Schmidt bases. Once the bases are known, Alice constructs her local measurements $\sigma_{z'} = |a\rangle\langle a| - |a_\perp\rangle\langle a_\perp|$ and $\sigma_{y'} = i|a_\perp\rangle\langle a| - i|a\rangle\langle a_\perp|$, and so does Bob in analogy. They can now detect entanglement with only two correlation measurements because $T_{z'z'}^2 + T_{y'y'}^2 = 1 + \sin^2 2\theta > 1$ for all pure entangled states. Note, the laboratories are not required to share a common reference frame.

In order to extract the Schmidt bases from experimental data, one starts with local measurements, determining the local Bloch vectors $\vec{\alpha}(\vec{\beta})$ of Alice (Bob). (Those vectors are related to the correlation tensor coefficients via $\alpha_i = T_{i0}/\sqrt{T_{x0}^2 + T_{y0}^2 + T_{z0}^2}$.) We consider two cases. First, suppose that a pure state has nonvanishing local Bloch vectors. Their directions define the Schmidt bases of Alice and Bob up to a global phase ϕ . Writing these bases in the computational basis

$$\begin{aligned} |a\rangle &= \cos\xi_A|0\rangle + e^{i\varphi_A}\sin\xi_A|1\rangle, \\ |a_\perp\rangle &= \sin\xi_A|0\rangle - e^{i\varphi_A}\cos\xi_A|1\rangle, \\ |b\rangle &= \cos\xi_B|0\rangle + e^{i\varphi_B}\sin\xi_B|1\rangle, \\ |b_\perp\rangle &= e^{i\phi}(\sin\xi_B|0\rangle - e^{i\varphi_B}\cos\xi_B|1\rangle), \end{aligned} \quad (3)$$

we see that the required coefficients can be inferred directly from the local Bloch vectors, $\vec{\alpha} = (\sin 2\xi_A \cos \varphi_A, \sin 2\xi_A \sin \varphi_A, \cos 2\xi_A)$ on Alice's side, and similarly for Bob. The global phase of $|b_\perp\rangle$ shows up as the relative phase in the decomposition (2); i.e., $|\psi_S\rangle = \cos\theta|a\rangle|b\rangle + \sin\theta e^{i\phi}|a_\perp\rangle|b_\perp\rangle$ (with $|b_\perp\rangle = e^{i\phi}|\tilde{b}_\perp\rangle$). It can be determined, for example, from the T_{yy} correlation as $\cos\phi = T_{yy}/\sqrt{1 - T_{x0}^2 - T_{y0}^2 - T_{z0}^2}$. If Bob would use the basis $\{|b\rangle, |\tilde{b}_\perp\rangle\}$ to build his observables $\sigma_{z''}$ and $\sigma_{y''}$, the corresponding correlations $T_{y'y''} = \sin 2\theta \cos\phi$ would vanish for $\cos\phi = 0$ and the two measurements $T_{z'z''}$ and $T_{y'y''}$ would not suffice to detect entanglement. In such a case, however, the other two correlations, $T_{x'z''}$ and $T_{y'x''}$, are nonzero, and can be used to reveal entanglement. Therefore, the determination of ϕ in the calibration is not essential if one accepts possibly one more correlation measurement.

Second, in the case of vanishing local Bloch vectors, the pure state under consideration $|\psi_m\rangle$ is maximally entangled and admits infinitely many Schmidt decompositions. In order to truly prove entanglement, Bob can thus freely choose some basis, say computational basis, for which the state will now be of the form $|\psi_m\rangle = \frac{1}{\sqrt{2}} \times (|a\rangle|0\rangle + |a_\perp\rangle|1\rangle)$. The basis of Alice can be found after *filtering* by Bob in his Schmidt basis: $F = |0\rangle\langle 0| + \varepsilon|1\rangle\langle 1|$. (For an actual implementation, see the experimental

section.) When Bob informs Alice that his detector behind the filter clicked, the initial state becomes

$$(\mathbb{1} \otimes F)|\psi_m\rangle \rightarrow \frac{1}{\sqrt{1 + \varepsilon^2}}(|a\rangle|0\rangle + \varepsilon|a_\perp\rangle|1\rangle). \quad (4)$$

Note that, due to filtering, a nonvanishing local Bloch vector emerges for Alice. Thus, the respective Schmidt basis can be found with the method described above and used for the evaluation of $T_{z'z'}^2 + T_{y'y'}^2$.

Decision tree.—Our second algorithm for entanglement detection does not even require calibration and also applies directly to mixed states. Alice and Bob choose three orthogonal local directions x , y , and z independently from each other and agree to only measure correlations along these directions. In Fig. 1 we show exemplarily which correlations should be measured in order to detect entanglement in a small number of steps. Starting with a measurement of T_{zz} , one continues along the solid (or dotted) arrow if the correlation is higher (or lower) than some threshold value (e.g., $1/2$ in Fig. 1). The tree is based on the principle of correlation complementarity [19–22]: in quantum mechanics there exist trade-offs for the knowledge of dichotomic observables with corresponding anti-commuting operators. For this reason, if the correlation $|T_{zz}|$ is big, correlations $|T_{zx}|$, $|T_{zy}|$, $|T_{xz}|$, and $|T_{yz}|$ have to be small, because their corresponding operators anticommute with the operator $\sigma_z \otimes \sigma_z$. Therefore, the next significant correlations have to lie in the xy plane of the correlation tensor, and thus the tree continues with a measurement of the T_{yy} correlation. This concept can be

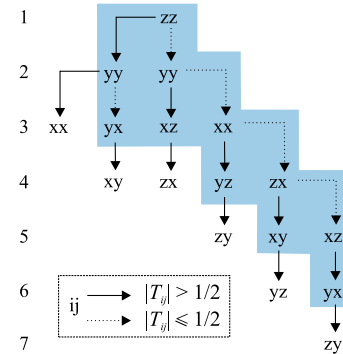


FIG. 1 (color online). The decision tree for efficient two-qubit entanglement detection. No shared reference frame is required between Alice and Bob; i.e., they choose their local x , y , z directions randomly and independently, which effectively gives rise to a basis $\{x_A, y_A, z_A\}$ for Alice and $\{x_B, y_B, z_B\}$ for Bob (not detailed in the figure or the main text). The scheme starts with measuring T_{zz} and follows at each step along the dashed arrow if the modulus of correlation is less than $\frac{1}{2}$ and otherwise along the continuous arrow. The algorithm succeeds as soon as $\sum T_{ij}^2 > 1$. The measurements in the blue shaded area suffice to detect all maximally entangled pure states with Schmidt-base vectors along x , y , or z .

generalized to multiqubit states. A decision tree for three qubits is given in the Supplemental Material [15]. The number of detected states grows with the number of steps through the decision tree. Since condition (1) is similar to the purity of a state, the scheme succeeds faster the more pure a state is (see Supplemental Material [15] for detailed analysis). Varying the threshold value does not lead to any significant changes in the statistic of detected states.

Finally, we connect both methods discussed here for the analysis of multiqubit states. A numerical simulation for pure states reveals that the correlation measurement along local Bloch vectors gives correlations close to the maximal correlations in more than 80% of cases. Therefore, these local directions give an excellent starting point for the decision tree.

Experiment.—For the demonstration of these new simple analysis methods we first use two photon-polarization entangled states. In the following, we will thus replace the computational basis states by horizontal ($|0\rangle \rightarrow |H\rangle$) and vertical ($|1\rangle \rightarrow |V\rangle$) linear polarization, respectively. The photon source (Fig. 2) is based on the process of spontaneous parametric down-conversion (SPDC), using a pair of crossed type I cut β -barium-borate (BBO) crystals pumped by a cw laser diode at a wavelength of $\lambda_{\text{pump}} = 402$ nm, with linear polarization of 45° . It emits pairs of horizontally and vertically polarized photons that superpose to the state $|\Psi\rangle = \frac{1}{\sqrt{2}}(|H\rangle|H\rangle + e^{i\delta}|V\rangle|V\rangle)$ [23]. The spectral bandwidth of the photons is reduced to 5 nm using interference filters, and two spatial emission modes are selected by coupling the photon pairs into two separate single-mode fibers.

For the purpose of preparing any pure two-qubit state, the polarization of each photon can be rotated individually by a set of quarter- (QWP) and half-wave plates (HWP) in each mode. By tilting an yttrium vanadate crystal (YVO_4) in front of the BBOs, the relative phase δ among the photon pairs can be set. Additionally, the state can be made asymmetric by removing a portion of vertically polarized light in one spatial mode with a Brewster plate

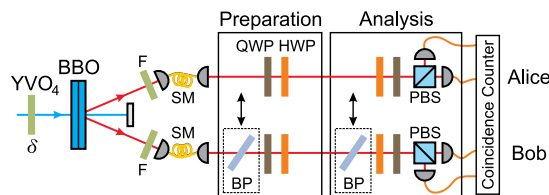


FIG. 2 (color online). Scheme of the experimental setup. The state $|\Psi\rangle = \frac{1}{\sqrt{2}}(|H\rangle|H\rangle + e^{i\delta}|V\rangle|V\rangle)$ is created by type I SPDC process. An yttrium vanadate crystal (YVO_4) is used to manipulate the phase δ of the prepared state. For preparation and analysis of the state, half- (HWP) and quarter-wave plates (QWP) are employed. Brewster plates (BP) can be introduced to make the state asymmetric and to perform the filter operation, respectively.

(BP). In the last step of the experiment, the polarization of each photon is analyzed with additional quarter- and half-wave plates and projection on $|H\rangle$ and $|V\rangle$ using a polarizing beam splitter (PBS). The local filtering of a maximally entangled state can be accomplished by placing a Brewster plate in front of the analysis wave plates. This Brewster plate reflects with a certain probability vertically polarized photons and, together with detection of a photon behind the Brewster plate, implements the filtering operation (4). Finally, the photons are detected by fiber-coupled single-photon detectors connected to a coincidence logic.

Experimental Schmidt decomposition.—Let us consider the state shown in Fig. 3(a). The protocol starts with Alice and Bob locally measuring the polarization of the photons, enabling them to individually determine the local Bloch vectors. For high efficiencies, which are possible in experiments with atoms or ions, the local measurements can indeed be done independently [24]. If nonvanishing local Bloch vectors can be identified, one can proceed to the next

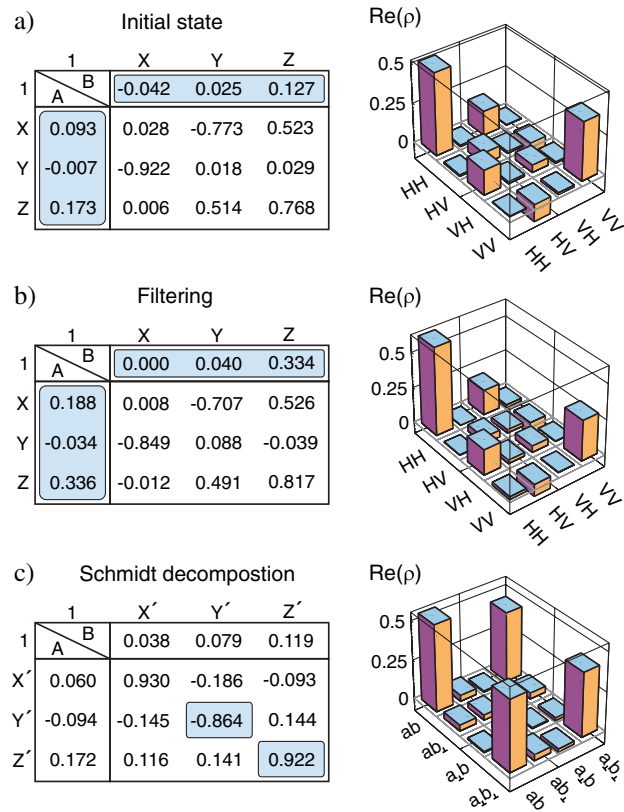


FIG. 3 (color online). Demonstration of Schmidt decomposition of a maximally entangled state prepared in unknown bases. The correlation tensor and corresponding density matrix are depicted for (a) the unknown state, (b) the state after applying local filtering, and (c) the state analyzed in the Schmidt bases. It is important to note that only the blue shaded elements of the correlation tensors will be measured, as this suffices to prove entanglement. The full correlation tensors and the corresponding states are only shown for completeness and didactic reasons.

step. For the example here, the local expectation values are close to zero and filtering has to be applied. By using a Brewster plate in front of Bob's analysis wave plate, local Bloch vectors emerge as long as the filtering operation is successful [Fig. 3(b)] [25]. In this case, we obtain $T_{0l} = (0.000, 0.040, 0.334)$ and $T_{k0} = (0.188, -0.034, 0.336)$.

In the next step, Alice and Bob use their local Bloch vectors to realign their analyzers to the new local Schmidt bases $\{|a\rangle, |a_{\perp}\rangle\}$ and $\{|b\rangle, |\tilde{b}_{\perp}\rangle\}$, respectively. This process diagonalizes the correlation tensor, as depicted in Fig. 3(c). Therefore, it is only necessary to measure $T_{z'z''} = 0.922 \pm 0.015$ and $T_{y'y''} = -0.864 \pm 0.015$ to prove entanglement, since $T_{z'z''}^2 + T_{y'y''}^2 = 1.597 \pm 0.038 > 1$. Hence, 2×3 local measurements are needed in the first step of the algorithm, three combined measurements are needed for filtering if necessary, and finally only two correlation measurements have to be performed for entanglement detection.

Application of the decision tree.—In order to demonstrate the application of the decision tree, we will apply it to three states. For the first state $\frac{1}{\sqrt{2}}(|H\rangle|H\rangle + |V\rangle|V\rangle)$, whose correlation tensor is depicted in Fig. 4(a), the decision tree (Fig. 1) starts with the measurement of the correlation $T_{zz} = 0.980 \pm 0.015$ and continues with $T_{yy} = -0.949 \pm 0.015$. These two measurements already prove entanglement since $T_{zz}^2 + T_{yy}^2 = 1.869 \pm 0.041 > 1$. For a second state, $\frac{1}{\sqrt{2}}(|R\rangle|R\rangle + i|L\rangle|L\rangle)$, we obtain a correlation of $T_{zz} = -0.056 \pm 0.015$, close to zero [Fig. 4(b)]. Consequently, the next steps according to our algorithm (Fig. 1) are to determine the correlation $T_{yy} = 0.978 \pm 0.015$, followed by $T_{xz} = -0.959 \pm 0.015$, with their squares adding up to

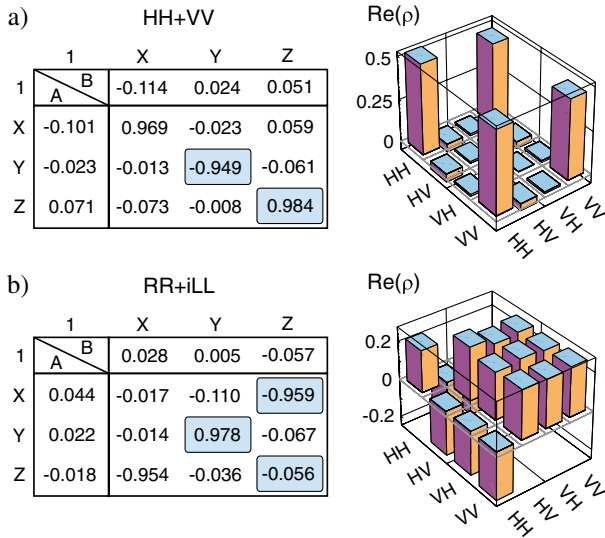


FIG. 4 (color online). Correlation tensors and density matrices of the experimental realization of two different states. The imaginary parts of the density matrices are negligible and therefore skipped. Using the decision tree, only the blue shaded correlations have to be measured for detecting entanglement. The errors of the correlations are <0.015 for (a) and <0.023 for (b).

a value of $1.879 \pm 0.041 > 1$ and hence proving entanglement. As a last example, we consider the initial state of Fig. 3. According to our decision tree, we need to measure $T_{zz} = 0.768 \pm 0.015$, $T_{yy} = 0.018 \pm 0.015$, and $T_{yx} = -0.922 \pm 0.015$, thus giving a value of $1.440 \pm 0.036 > 1$ and proving entanglement with only three steps.

Many qubits.—For the demonstration of multiqubit entanglement detection, we use two three-photon, polarization-entangled states: the W state [26] and the G state [27] (Fig. 5). In order to observe these states, a collinear type II SPDC source is used together with a linear setup to prepare the four-photon Dicke state $D_4^{(2)}$ [28,29]. Once the first photon is measured to be vertically polarized, the other three photons are projected into the W state. Similarly, the three-photon G state is obtained if the first photon is measured to be $+45^\circ$ polarized.

The protocol for entanglement detection starts with observers locally measuring the polarization of the photons, enabling them to individually determine the local Bloch vectors. For the G state we obtain $T_{i00} = (0.636, -0.008, -0.015)$, $T_{0j0} = (0.623, -0.092, 0.010)$, and $T_{00k} = (0.636, 0.070, 0.022)$. The local Bloch vectors suggest that the correlation T_{xxx} is big. Therefore, the decision tree starts with the measurement of $T_{xxx} = 0.904 \pm 0.025$ and continues with $T_{xzz} = -0.578 \pm 0.025$ (see Fig. 2 in the Supplemental Material [15]). These two measurements already prove entanglement because $T_{xxx}^2 + T_{xzz}^2 = 1.152 \pm 0.038 > 1$. For the W state, the local Bloch vectors $T_{i00} = (0.016, -0.070, 0.318)$, $T_{0j0} = (-0.010, -0.073, 0.308)$, and $T_{00k} = (-0.011, -0.0547, 0.319)$ suggest that now the correlation T_{zzz} is big. Indeed, we observe $T_{zzz} = -0.882 \pm 0.025$. The decision tree is the same as above but with local axes renamed as follows: $x \rightarrow z \rightarrow y \rightarrow x$. Therefore, the second measurement has to be T_{zyy} . With $T_{zyy} = 0.571 \pm 0.025$, we again prove entanglement as $T_{xxx}^2 + T_{zyy}^2 = 1.104 \pm 0.037 > 1$.

Conclusions.—We discussed and experimentally implemented two methods for fast entanglement detection for states about which we have no *a priori* knowledge. They are well suited for quantum communication schemes as the parties do not have to share a common reference frame, making the scheme insensitive to a rotation of the qubits during their transmission to the distant laboratories.

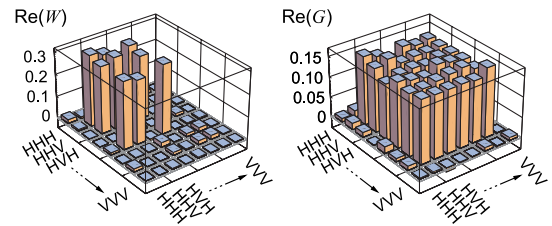


FIG. 5 (color online). Density matrices of the experimental realization of the G and W state. The corresponding fidelities are equal to 92.23% and 89.84%.

The two methods use a particularly simple and practical entanglement identifier [11]. One of them can be seen as experimental Schmidt decomposition and the other establishes a sequence of correlation measurements, leading to entanglement detection in a small number of steps.

We thank M. Żukowski for stimulating discussions. This work is supported by the EU project QESSENCE, the DAAD/MNiSW, the DFG-Cluster of Excellence MAP, and by the National Research Foundation and Ministry of Education in Singapore. W.L. is supported by the MNiSW Grant No. N202 208538 and by the Foundation for Polish Science. CS thanks QCCC of the Elite Network of Bavaria for support.

-
- [1] M. A. Nielsen and I. Chuang, *Quantum Computation and Quantum Information* (Cambridge University Press, Cambridge, 2000).
- [2] R. Horodecki, P. Horodecki, M. Horodecki, and K. Horodecki, *Rev. Mod. Phys.* **81**, 865 (2009).
- [3] A. Peres, *Phys. Rev. Lett.* **77**, 1413 (1996).
- [4] M. Horodecki, P. Horodecki, and R. Horodecki, *Phys. Lett. A* **223**, 1 (1996).
- [5] M. Bourennane, M. Eibl, C. Kurtsiefer, S. Gaertner, H. Weinfurter, O. Gühne, P. Hyllus, D. Bruß, M. Lewenstein, and A. Sanpera, *Phys. Rev. Lett.* **92**, 087902 (2004).
- [6] B. M. Terhal, *Phys. Lett. A* **271**, 319 (2000).
- [7] M. Lewenstein, B. Kraus, J. I. Cirac, and P. Horodecki, *Phys. Rev. A* **62**, 052310 (2000).
- [8] D. Bruss, J. I. Cirac, P. Horodecki, F. Hulpke, B. Kraus, M. Lewenstein, and A. Sanpera, *J. Mod. Opt.* **49**, 1399 (2002).
- [9] O. Gühne and P. Hyllus, *Int. J. Theor. Phys.* **42**, 1001 (2003).
- [10] O. Gühne and G. Toth, *Phys. Rep.* **474**, 1 (2009).
- [11] P. Badziąg, Č. Brukner, W. Laskowski, T. Paterek, and M. Żukowski, *Phys. Rev. Lett.* **100**, 140403 (2008).
- [12] E. Schmidt, *Math. Ann.* **63**, 433 (1907).
- [13] A. Peres, *Quantum Theory: Concepts and Methods* (Kluwer Academic, Dordrecht, 1995).
- [14] R. Horodecki, P. Horodecki, and M. Horodecki, *Phys. Lett. A* **210**, 377 (1996).
- [15] See Supplemental Material at <http://link.aps.org/supplemental/10.1103/PhysRevLett.108.240501> for more details on the efficiency of the method based on the decision tree for pure and mixed states of two qubits and an algorithm that constructs the tree for many qubits.
- [16] W. Laskowski, M. Markiewicz, T. Paterek, and M. Żukowski, *Phys. Rev. A* **84**, 062305 (2011).
- [17] Although the effort to evaluate (1) generally scales as the one for full state tomography, we can directly evaluate the criterion from raw data without any further numerics required to reconstruct a physical density matrix [18].
- [18] D. F. V. James, P. G. Kwiat, W. J. Munro, and A. G. White, *Phys. Rev. A* **64**, 052312 (2001).
- [19] P. Kurzyński, T. Paterek, R. Ramanathan, W. Laskowski, and D. Kaszlikowski, *Phys. Rev. Lett.* **106**, 180402 (2011).
- [20] G. Toth and O. Gühne, *Phys. Rev. A* **72**, 022340 (2005).
- [21] S. Wehner and A. Winter, *J. Math. Phys. (N.Y.)* **49**, 062105 (2008).
- [22] S. Wehner and A. Winter, *New J. Phys.* **12**, 025009 (2010).
- [23] P. G. Kwiat, E. Waks, A. G. White, I. Appelbaum, and P. H. Eberhard, *Phys. Rev. A* **60**, R773 (1999).
- [24] Due to the low efficiency of the SPDC setup we have to use coincidence counts here. Using only the single counts, the local Bloch vector of Alice is slightly different. In this example we obtain $T_{0l} = (-0.073, -0.091, -0.059)$ and $T_{k0} = (0.031, 0.041, 0.037)$.
- [25] This in consequence means, that for the filtering Alice and Bob have to communicate with each other and hence this measurement is *not* local.
- [26] $|W\rangle = (|HHV\rangle + |HVH\rangle + |VHH\rangle)/\sqrt{3}$; W. Dür, G. Vidal, and J. I. Cirac, *Phys. Rev. A* **62**, 062314 (2000).
- [27] $|G\rangle = (|W\rangle + |\bar{W}\rangle)/\sqrt{2}$, where $|\bar{W}\rangle = (|VVH\rangle + |HVV\rangle + |VHV\rangle)/\sqrt{3}$; A. Sen(De), U. Sen, and M. Żukowski, *Phys. Rev. A* **68**, 032309 (2003).
- [28] $|D_4^{(2)}\rangle = (|HHVV\rangle + |HVHV\rangle + |VHHV\rangle + |HVVH\rangle + |VHVH\rangle + |VVHH\rangle)/\sqrt{6}$; R. Krischek, C. Schwemmer, W. Wieczorek, H. Weinfurter, P. Hyllus, L. Pezze, and A. Smerzi, *Phys. Rev. Lett.* **107**, 080504 (2011).
- [29] N. Kiesel, C. Schmid, G. Toth, E. Solano, and H. Weinfurter, *Phys. Rev. Lett.* **98**, 063604 (2007).